

# Benchmark case ”*FSAI-01: A benchmark case for aeroacoustic simulations involving fluid-structure-acoustic interaction transferred from the process of human phonation*” – Data description

Stefan Schoder, Sebastian Falk, Andreas Wurzinger, Alexander Lodermeier,  
Stefan Becker, Stefan Kniesburges

## Contact:

stefan.schoder@tugraz.at  
stefan.kniesburges@uk-erlangen.de

## 1 Introduction

This document includes the description of the data provided for the aeroacoustic benchmark case that is introduced in Schoder et al.: *A benchmark case for aeroacoustic simulations involving fluid-structure-acoustic interaction transferred from the process of human phonation*. [7] published in *Acta Acustica*, DOI: ... .

The benchmark case was transferred from a synthetic larynx and includes a large amount of experimental data of the fluid flow, the periodical dynamics of the silicone vocal folds and the produced sound field. These data are shown in tab. 1.

Data set	VeF	$f_0$	$\bar{P}_{sub}$	Q	Measuring data
Acoustic & aerodynamic pressure		143 Hz	3251 Pa	100l/min	sub- & supraglottal pressure @ 40 positions
	✓	148 Hz	2449 Pa	70l/min	sound pressure far field @ 4 positions
Visualization VFs dynamics		145 Hz	3667 Pa	100l/min	subglottal pressure
	✓	148 Hz	2754 Pa	75l/min	high-speed footage
Flow field PIV		146 Hz	3322 Pa	95l/min	2D flow field mid-coronal plane subglottal pressure

Table 1: Measuring data sets of *synthVOICE* for validation [2, 1, 3, 4, 6, 5], with  $f_0$  being the fundamental frequency,  $\bar{P}_{sub}$  the subglottal pressure and  $Q$  the flow rate. The presence of the VeFs are indicated by the checkmark symbol ✓.

## 2 Acoustic and aerodynamic pressures

- Synchronous sampling
- Frame rate:  $f_s = 44.1$  kHz
- Measuring duration / number samples:  $T = 60$  s /  $N = 2.646$  Mio
- Resolution aerodynamic pressures: 16 bit
- Resolution acoustic pressures: 24 bit
- File format: Space separated ASCII, UTF-8

- 20 • Files subglottal pressure, figure 1:
- 21 – Without ventricular folds: [aerodynamic\\_pressure\\_subglottal.dat](#)
- 22 – With ventricular folds (VeFs): [aerodynamic\\_pressure\\_subglottal\\_VeFs.dat](#)
- 23 • Files supraglottal pressure, figure 1:
- 24 – Without ventricular folds:
- 25 \* top wall: [aerodynamic\\_pressure\\_supraglottal\\_top.dat](#)
- 26 \* back wall: [aerodynamic\\_pressure\\_supraglottal\\_back.dat](#)
- 27 \* bottom wall: [aerodynamic\\_pressure\\_supraglottal\\_bottom.dat](#)
- 28 – With ventricular folds (VeFs): [aerodynamic\\_pressure\\_subglottal\\_VeFs.dat](#)
- 29 \* top wall: [aerodynamic\\_pressure\\_supraglottal\\_VeFs\\_top.dat](#)
- 30 \* back wall: [aerodynamic\\_pressure\\_supraglottal\\_VeFs\\_back.dat](#)
- 31 \* bottom wall: [aerodynamic\\_pressure\\_supraglottal\\_VeFs\\_bottom.dat](#)
- 32 • Files sound pressure, figure 2 and 3:
- 33 – Without ventricular folds: [acoustic\\_pressure.dat](#)
- 34 – With ventricular folds (VeFs): [acoustic\\_pressure\\_VeFs.dat](#)

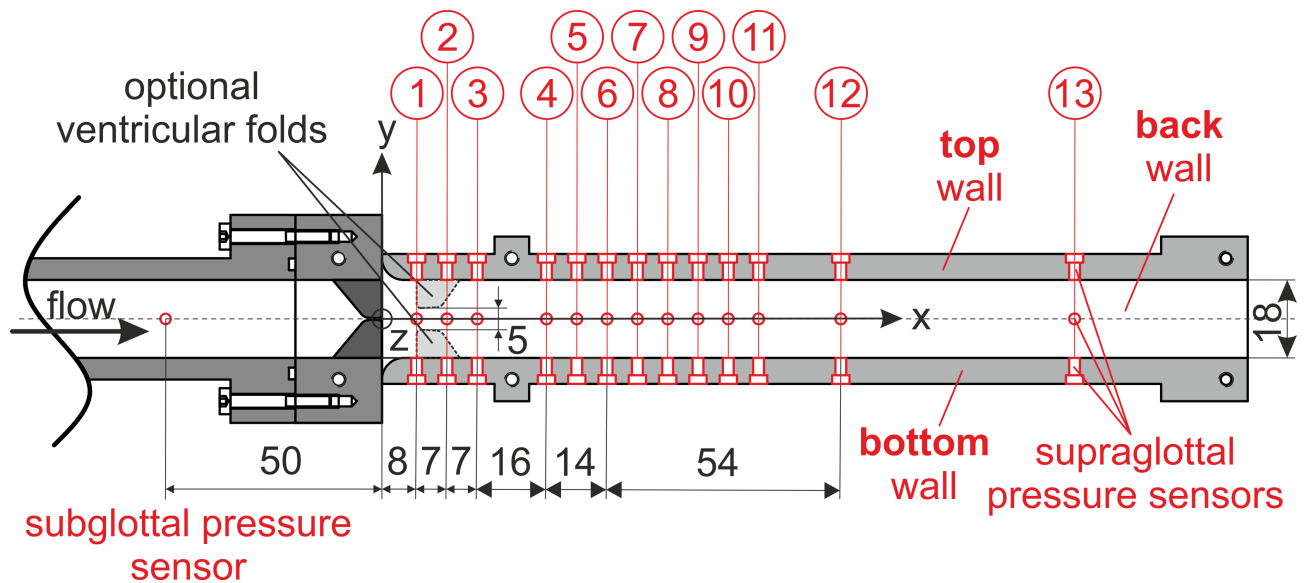


Figure 1: Synthetic larynx model and supraglottal channel with optional ventricular folds (VeF) from side perspective. The positions of the subglottal pressure sensor and the 39 supraglottal pressure sensors are indicated in red. The z-dimension of the channel cross-section amounts 15 mm. All dimensions in mm

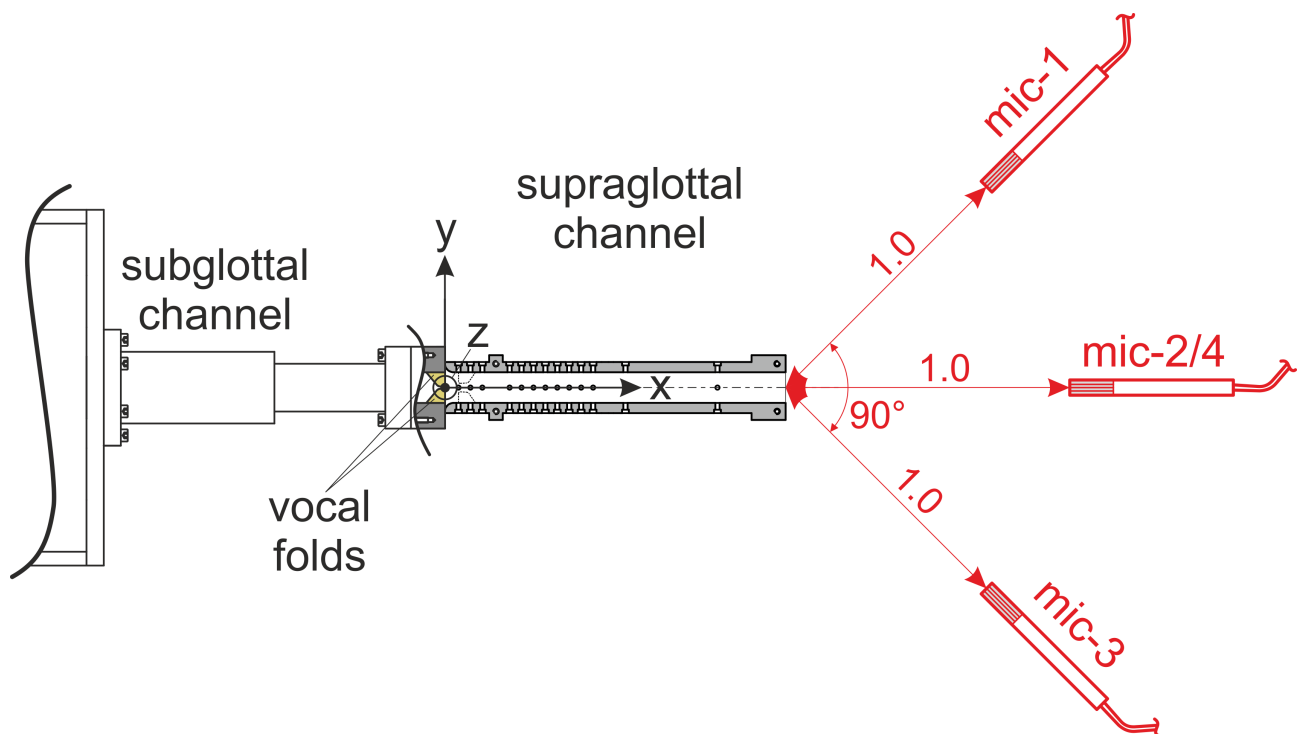


Figure 2: Synthetic larynx model and supraglottal channel with optional ventricular folds (VeF) from side perspective (xy). The position of the four microphones are shown in red. All dimensions in mm.

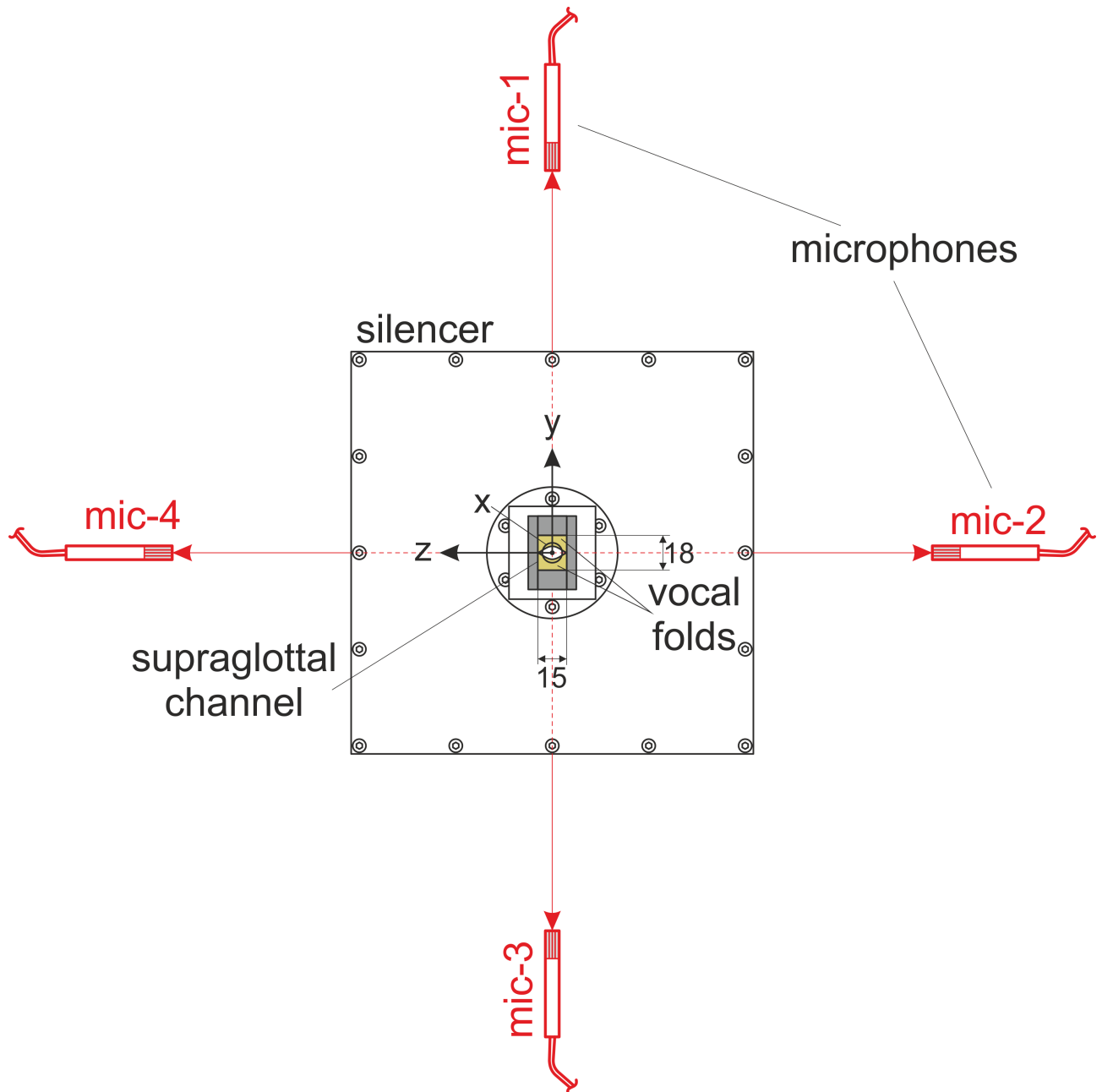


Figure 3: Synthetic larynx model and supraglottal channel with optional ventricular folds (VeF) from front perspective ( $yz$ ). The position of the four microphones are shown in red. All dimensions in mm.

### 3 High-speed visualization of the vocal fold dynamics

- Aerodynamic subglottal pressure:
  - Sampling rate:  $f_s = 100$  kHz
  - Measuring duration / number samples:  $T_s = 0.125$  s /  $N_s = 12\,500$
  - Resolution aerodynamic pressures: 16 bit
  - File format: Space separated ASCII, UTF-8
  - Files aerodynamic subglottal pressure, figure 4:
    - \* Without ventricular folds: [aerodynamic\\_pressure\\_subglottal\\_HS.dat](#)
    - \* With ventricular folds (VeFs): [aerodynamic\\_pressure\\_subglottal\\_VeFs\\_HS.dat](#)
- High-speed visualization:
  - Frame rate:  $f_f = 4$  kHz
  - Recording duration / number frames:  $T_s = 0.125$  s /  $N_f = 500$
  - Image resolution & scale factor:
    - \* Without VeFs:  $I_R = 512 \times 512$  pixel &  $S = 6.3 \cdot 10^{-3}$  mm<sup>2</sup>/pixel
    - \* With VeFs:  $I_R = 1024 \times 1024$  pixel &  $S = 5.78 \cdot 10^{-3}$  mm<sup>2</sup>/pixel
  - Results types: glottis contour, glottis area waveform
  - File format: Space separated ASCII, UTF-8
  - Files glottis contour, figure 4:
    - \* Without ventricular folds: [glottis\\_contour\\_coordinates\\_HS.snake](#)
    - \* With ventricular folds (VeFs): [glottis\\_contour\\_coordinates\\_VeFs\\_HS.snake](#)
  - Files glottis area waveform, figure 4:
    - \* Without ventricular folds: [glottis\\_area\\_waveform\\_HS.dat](#)
    - \* With ventricular folds (VeFs): [glottis\\_area\\_waveform\\_VeFs\\_HS.dat](#)

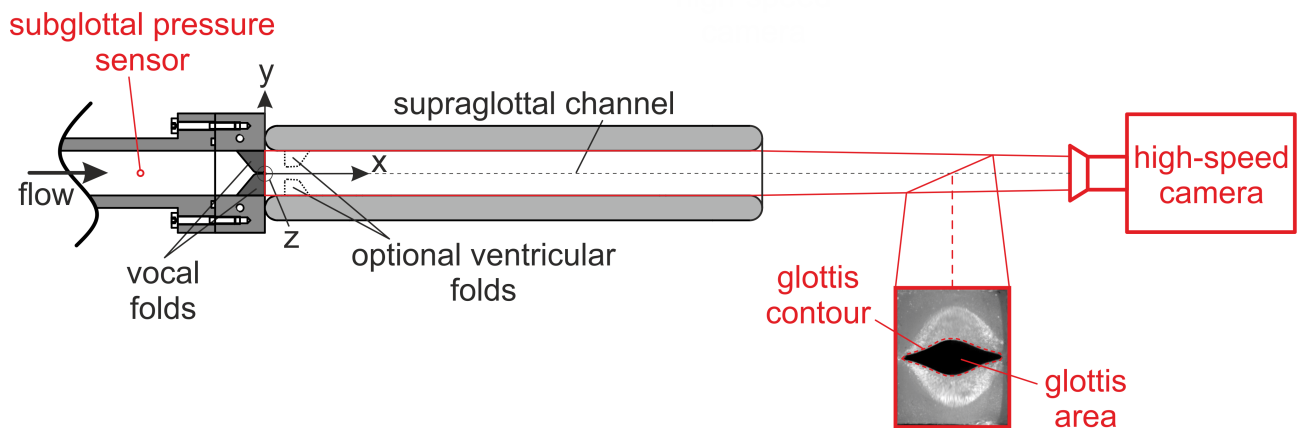


Figure 4: Synthetic larynx model and supraglottal channel with optional ventricular folds (VeF) from side perspective with high-speed camera to visualize the vocal fold dynamics. The recorded perspectives is shown for one instance. The measured signals are indicated in red.

## 4 High-speed PIV measurements of the flow field downstream of the vocal folds

- Aerodynamic subglottal pressure:
  - Sampling rate:  $f_s = 96$  kHz
  - Measuring duration / number samples:  $T_s = 10$  s /  $N_s = 960\,000$
  - Resolution aerodynamic pressures: 16 bit
  - File format: Space separated ASCII, UTF-8
  - Files aerodynamic subglottal pressure, figure 5:
    - \* Without ventricular folds: [aerodynamic\\_subglottal\\_pressure\\_PIV.dat](#)
- High-speed PIV flow field data:
  - Sample rate:  $f_f = 10$  kHz
  - Recording duration / number frames:  $T_s = 3.277$  s /  $N_s = 32\,767$
  - Region of interest (ROI):  $39 \times 18$  mm<sup>2</sup>
  - Pixel-resolution ROI:  $76 \times 24$  pixel
  - File format: Space separated ASCII, UTF-8
  - Files [2D-2C PIV flow field data](#), figure 5:
    - \* Without ventricular folds: [pic\\_#n.dat](#)
    - \*  $\#n=1-N$  with increment 2 and maximum sample  $N$ : increasing time step  $\Delta t = 10^{-4}$  s.
    - \* Tecplot file format, detailed readable header in each file

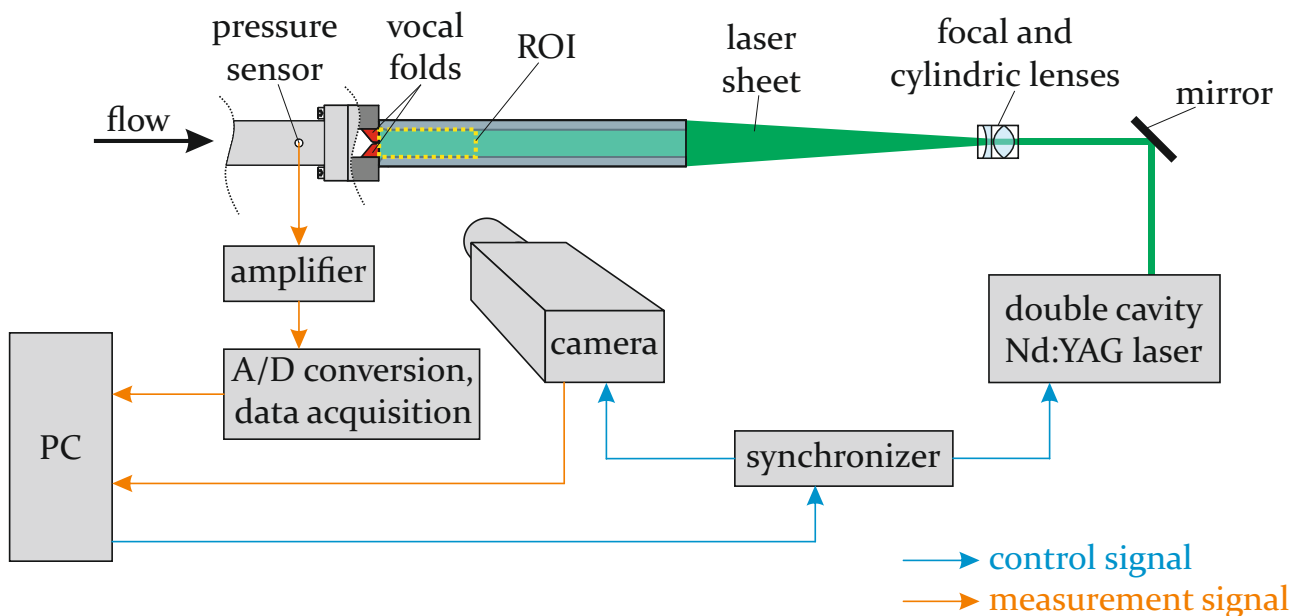


Figure 5: Synthetic larynx model and supraglottal channel without ventricular folds (VeF) from side perspective within the high-speed PIV measuring setup. The region of interest (ROI) is directly downstream of the vocal folds.

## References

- [1] S. Kniesburges. *Fluid-Structure-Acoustic Interaction during Phonation in a Synthetic Larynx Model*. phdthesis, FAU Erlangen-Nürnberg, Düren, 2014. 77  
78  
79
- [2] S. Kniesburges, C. Hesselmann, S. Becker, E. Schlücker, and M. Döllinger. Influence of vortical flow structures on the glottal jet location in the supraglottal region. *J Voice*, 272(5):531–544, 2013. 80  
81
- [3] Stefan Kniesburges, Veronika Birk, Alexander Lodermeier, Anne Schützenberger, Christopher Bohr, and Stefan Becker. Effect of the ventricular folds in a synthetic larynx model. *Journal of Biomechanics*, 55:128–133, April 2017. 82  
83
- [4] Stefan Kniesburges, Alexander Lodermeier, Marion Semmler, Yvonne Katrin Schulz, Anne Schützenberger, and Stefan Becker. Analysis of the tonal sound generation during phonation with and without glottis closure. *The Journal of the Acoustical Society of America*, 147(5):3285–3293, May 2020. 84  
85  
86
- [5] A. Lodermeier, Eman Bagheri, S. Kniesburges, C. Näger, J. Probst, M. Döllinger, and S. Becker. The mechanisms of harmonic sound generation during phonation: A multi-modal measurement-based approach. *J Acoust Soc Am*, 150(5):3485–3499, 2021. 87  
88  
89
- [6] A. Lodermeier, M. Tautz, S. Becker, M. Döllinger, V. Birk, and S. Kniesburges. Aeroacoustic analysis of the human phonation process based on a hybrid acoustic piv approach. *Exp Fluids*, 59:13, 2018. 90  
91
- [7] S. Schoder, S. Falk, A. Wurzinger, A. Lodermeier, S. Becker, and S. Kniesburges. A benchmark case for aeroacoustic simulations involving fluid-structure-acoustic interaction transferred from the process of human phonation. *Acta Acustica*, in press, 2023. 92  
93  
94